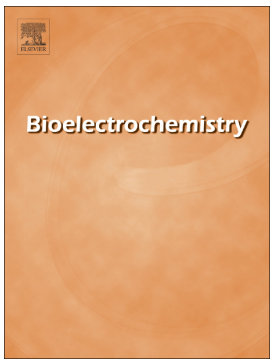

A novel impedance enhancer for amperometric biosensor based ultrasensitive detection of matrix metalloproteinase-2

Huiqiang Wang, Zhanfang Ma, Hongliang Han

PII: S1567-5394(19)30201-4
DOI: https://doi.org/10.1016/j.bioelechem.2019.06.009
Reference: BIOJEC 7324

To appear in: *Bioelectrochemistry*

Received date: 23 March 2019
Revised date: 24 June 2019
Accepted date: 24 June 2019

Please cite this article as: H. Wang, Z. Ma and H. Han, A novel impedance enhancer for amperometric biosensor based ultrasensitive detection of matrix metalloproteinase-2, Bioelectrochemistry, https://doi.org/10.1016/j.bioelechem.2019.06.009

A novel impedance enhancer for amperometric biosensor based ultrasensitive detection of matrix metalloproteinase-2

Huiqiang Wang[a,b,c], Zhanfang Ma[a]*, Hongliang Han[a]*

[a] Department of Chemistry, Capital Normal University, Beijing 100048, China

[b] Beijing National Laboratory for Molecular Sciences (BNLMS), Key Laboratory of Green Printing, Institute of Chemistry, Chinese Academy of Sciences, Zhongguancun North First Street 2, Beijing 100190, China

[c] University of Chinese Academy of Sciences, Beijing 100049, China

*Corresponding Author: Email: mazhanfang@cnu.edu.cn (Ma ZF); hanhongliang@cnu.edu.cn (Han HL)

Abstract

The detection range and sensitivity is crucial to the determination of tumor markers. For amperometric biosensors, the detection range relies on the initial current signals (I_0) and the sensitivity is tightly related to the current signals difference (ΔI) caused by per unit concentration target. Herein, an amperometric biosensor was fabricated using polyaniline gel as substrate and CS-AuNPs-Pb^{2+} as impedance enhancer. The sensing substrate exhibited strong current signal in $[Fe(CN)_6]^{3-/4-}$ due to the excellent conductivity and large specific surface area of polyaniline gel. CS-AuNPs-Pb^{2+} with large hindrance effect can significantly increase interfacial resistance, resulting in the enhancement of ΔI. In addition, Pb^{2+} can react with sodium tartrate to produce non-conducting sodium tartrate gel on sensing interface, leading to further amplification of ΔI. Matrix metalloproteinase-2 (MMP-2) was analyzed to prove the feasibility of this strategy. The proposed amperometric biosensor reveal both wide linear detection range from 1 pg mL^{-1} to 1 μg mL^{-1} and high sensitivity of 28.4 $\mu A \cdot (LgC_{MMP\text{-}2})^{-1}$. Therefore, this strategy will be of great significance to design other ultrasensitive amperometric biosensors.

Keywords: impedance enhancer; sodium tartrate gel; amperometric biosensor; polyaniline gel; carbon sphere; matrix metalloproteinase-2

1. Introduction

Matrix metalloproteinase-2 (MMP-2) is a zinc-dependent proteinase which is capable of degrading extracellular matrix proteins, and its levels in serum are correlated to the occurrence and growth of colorectal, bladder and breast cancers [1-6]. Therefore, developing rapid and sensitive methods for the detection of MMP-2 is crucial in early clinical diagnosis.

Recently, numerous techniques including electrochemical, fluorescence and bioluminescence assays have been used for sensitive detection of MMP-2 [1,2,32]. Among these methods, electrochemical biosensors have shown significant advantages due to its high sensitivity, low cost, and easy preparation. In electrochemical assay, the sensitivity is defined as the current signal difference (ΔI) between an immunosensor treated with and without treatment with per unit concentration target [7-10]. A variety of effective strategies have been implemented to elevate ΔI of an electrochemical biosensor via the enrichment of redox species, employment of conductive nanomaterials, and catalytic amplification [11-15]. However, two major obstacles exist: Firstly, the ΔI is small, thus, the small variations of MMP-2 level cannot be sensitively monitored. Secondly, the initial current signals (I_0) are relatively low, commonly several tens μA, leading to a narrow linear detection range. [16-21]. Therefore, developing biosensors with strong initial current signals and large ΔI is of great significance to achieve wide detection range and high sensitivity [22-27].

In this work, an amperometric biosensor was developed using polyaniline gel as the substrate and Pb^{2+} loaded carbon spheres (CS)-gold nanoparticles nanocomposites (CS-AuNPs-Pb^{2+}) as a novel impedance enhancer. Due to the excellent conductivity and large specific surface area of polyaniline gel, the gel based sensing substrate provides a strong I_0 (720 μA) in $[Fe(CN)_6]^{4-/3-}$, which guarantees wide detectable

range. CS-AuNPs-Pb^{2+} with large hindrance effect can significantly increase interfacial resistance, resulting in the enhancement of ΔI. In addition, Pb^{2+} can react with sodium tartrate to produce non-conducting sodium tartrate gel on sensing interface, leading to further amplification of ΔI. Benefits from the polyaniline gel and CS-AuNPs-Pb^{2+} impedance enhancer, a strong initial current signals and large ΔI was obtained, and the as-prepared biosensor shows a wide linear detection range and high sensitivity for the determination of MMP-2.

2. Experimental

All materials and reagents and apparatus were placed in Electronic supplementary material.

2.1. Synthesis of CS-AuNPs-Pb

To prepare carbon nanosphere (CS), 20 mL glucose (60 mM) was kept at 170 °C for 6 h. Then, the above solutions were collected via centrifugation at 8000 rpm for 10 min and washed with ethanol five times. The obtained CS was redispersed in 5 mL ultrapure water for further use. $HAuCl_4$ (50μL, 5 mM) and ascorbic acid (20 μL, 5 mM) were added into the above solution successively and stirred for 30 min to obtain AuNPs-CS composites. After collected by centrifugation, the composites were washed with water several times and diluted with 5.00 mL ultrapure water. $Pb(NO_3)_2$ (5 wt%) was added into the above solution then stirred for 60 min. The CS-AuNPs-Pb nanoparticles were gained via centrifugation, washed with water five times, and diluted with 5.00 mL ultrapure water.

2.2. Fabrication of the electrochemical biosensor substrate

Firstly, a glassy carbon electrode (GCE) with a diameter of 4 mm was polished using 0.05 μm alumina polishing powder. The working electrode was immersed in 1 M KCl solution (20 mL) containing 0.15 M phytic acid (2 mL) and 0.5 M aniline (1

mL). Then, the polyaniline gel on the surface of GCE was electrodeposited at potentiostatic 0.8 V. AuNPs were electrodeposited on the polyaniline gel modified electrodes by amperometric i-t curve technique at -0.2 V for 30 s in 0.5 mM $HAuCl_4$ containing 0.1 M KCl solutions. After washing, peptide (NH_2-Gly-Gly-Lys-Gly-Arg-Val-Gly-Leu-Pro-Gly-Cys-SH) (80 μL, 70 μM) solutions ware added onto the modified electrode and incubated at 37 °C for 4 h. Subsequently, CS-AuNPs-Pb was added onto the peptide-Au/PANI/GCE and fixed at 37 °C for 5 h. Glutathione was used as the blocking buffer to eliminate nonspecific binding sites of the CS-AuNPs-Pb. After washing, the electrochemical biosensor substrate was obtained. The CS-AuNPs-Pb/peptide/AuNPs/polyaniline gel/GCE was incubated with 20 μL MMP-2 at various concentrations at 37 °C for 60 min. Next, sodium tartrate (2 mM) was introduced to react with the Pb^{2+}, producing a sodium tartrate gel with greater impedance.

2.3. Electrochemical measurement

To investigate the detection process, detection process, a sequence of standard solutions of MMP-2 with different concentrations was fixed on the sensing platform at 37 °C. The modified electrode was covered with 2.0 mM ST acetate buffer solution (pH = 6.0) at 37 °C for 45 min, which was then carefully washed. Subsequently, square wave voltammetry (SWV) measurements were performed from -0.2 to 0.6 V in 0.01 M phosphate buffered solution.

3. Results and Discussion

3.1. Choice of Materials

The polyaniline gel with good conductivity and large specific surface area was electrodeposited on the surface of GCE to produce a strong I_0 in $[Fe(CN)_6]^{4-/3-}$ (720 μA, which is ten-fold higher than those of previous works), providing wide detectable

range. AuNPs, possessing good conductivity, were electrodeposited onto the polyaniline gel to immobilize the peptide. CS-AuNPs-Pb nanocomposites, as the impedance enhancer, then linked with the peptides through the interaction between AuNPs on enhancer and the amino group of the peptide. The carbon spheres can increase ΔI due to their poor conductivity and can absorb abundant Pb^{2+} via electrostatic interaction. Then, Pb^{2+} reacts with introduced sodium tartrate (ST) to produce a sodium tartrate gel with greater impedance, resulting in the further enhancement of ΔI. Glutathione was also added to avoid the unspecific adsorption between MMP-2 and the active sites of AuNPs in the CS-AuNPs-Pb composite, which further increases impedance. Since MMP-2 can specifically recognize and cleave the peptides (NH_2-Gly-Gly-Lys-Gly-Arg-Val-Gly-Leu-Pro-Gly-Cys-SH), the fabricated biosensor exhibits a wide linear range and high sensitivity for MMP-2.

Schematic 1

3.2. Characterization of CS, CS-AuNPs, and CS-AuNPs-Pb

The morphologies and sizes of CS, CS-AuNPs, and CS-AuNPs-Pb were investigated by transition electron microscopy (TEM) **(Fig. 1A-C)**. CS displayed a smooth surface and was about 200 nm in diameter **(Fig. 1A)**. CS-AuNPs was fabricated by the in situ formation of gold nanoparticles, which were ca. 10 nm and densely distributed on CS **(Fig. 1B)**. The CS-AuNPs-Pb composite displayed uniform morphology and was about 210 nm in diameter **(Fig. 1C)**. The detailed compositions of CS, CS-AuNPs, and CS-AuNPs-Pb were further characterised by X-ray photoelectron spectroscopy (XPS) **(Fig. 1D-F)**. As shown in Fig. 1D-F, the C1s and O1s peaks correspond to CS, while the Au4f peaks of CS-AuNPs and CS-AuNPs-Pb are assigned to the reduced gold **(Fig. 1E, F)**. For the CS-AuNPs-Pb composite, the Pb4f peaks belonged to Pb^{2+} **(Fig. 1F)**.

Zeta potential measurements were obtained to confirm the adsorption process of Pb^{2+} by CS. The zeta potentials of CS and CS-AuNPs were -38 and -26 mV **(Fig. S1A; Fig. S2A, B)**, respectively. After adsorption of Pb^{2+}, the zeta potential of CS-AuNPs-Pb was 8 mV **(Fig. S1A**; **Fig. S2C)**, indicating that Pb^{2+} was successfully adsorbed on CS. Compared with the CS-AuNPs-modified GCE (0 μA) (curve a), a high current signal (-0.48 V, 340 μA, the characteristic peak of Pb^{2+}) (curve b) was produced by the CS-AuNPs-Pb-modified GCE **(Fig. S1B)**. It further indicated that Pb^{2+} was successfully adsorbed by CS.

Fig. 1

3.3. Proof tests of the construction procedures

To investigate the construction procedures (the ST-gel/CS-AuNPs-Pb/peptides/AuNPs/PAn-gel/GCE) for MMP-2 detection, scanning electrode microscopy (SEM) images were obtained. Fig. 2A presents the unmodified bare GCE, while Fig. 2B and C shows that the 3D network structures of PANI gel and AuNPs/PANI gel. The morphology of the electrode surface was almost unchanged after immobilization of the peptides (**Fig. 2D**), and CS-AuNPs-Pb composites were densely distributed on the surface of CS-AuNPs-Pb/peptides/AuNPs/PAn-gel/GCE (**Fig. 2E**). After introduction of CS-AuNPs-Pb and the reaction between sodium tartaric and Pb^{2+}, the poorly conductive sodium tartaric gel (ST-gel) formed on the surface of the modified electrode (**Fig. 2F**).

Fig. 2

The fabrication procedures of the biosensor were investigated by electrochemical impedance spectroscopy (EIS) (**Fig. 3A)** and square wave voltammetry (SWV) (**Fig. 3B**) in 0.01 M phosphate buffered solution with 5.0 mM $[Fe(CN)_6]^{4-/3-}$ and 0.1 M KCl (pH 7.4). The tendencies of electron-transfer resistance in the EIS plots were

consistent with the SWV measurement results. In the SWV plots, a high current signal (720 μA) (curve b) was observed by the GCE modified with PANI gel in 5.0 mM $[Fe(CN)_6]^{4-/3-}$ solutions. In contrast, only 210 μA was obtained for the bare GCE under the same conditions (curve a). This difference can be explained by the enhanced current signal due to AuNPss on the electrode, which exhibit excellent conductivity and a large specific surface area (curve c). The current signal decreased when peptides were incubated on the AuNPs/PAn-gel/GCE (curve d), indicating that the peptides were successfully fixed. When the peptides/AuNPs/PAn-gel/GCE was treated with CS-AuNPs-Pb (curve e) and glutathione (curve f), the peak current further decreased, which were attributable to the poor conductivity of CS-AuNPs-Pb and glutathione. After incubation of MMP-2, the current signal increased (curve g) since the peptide was cleaved by MMP-2, and the SWV signal dramatically decreased after precipitation of the ST-gel (curve h). In addition, the different shapes of the signal during the fabrication procedures of the biosensor can be explained by the following reasons: (1) The wider SWV signal of the electrode with polyaniline gel was composed of an acromion at 0.24 V produced by $[Fe(CN)_6]^{4-/3-}$ and a wide current signal at 0.4 V generated from polyaniline. In this case, the wider SWV signal at about 0.4 V was synergetic effect related to the SWV signals of $[Fe(CN)_6]^{4-/3-}$ (0.24 V) and polyaniline (0.2 V and 0.4 V) [28], respectively. (2) The impendence will be changed during the fabrication procedures of the biosensor, which can lead to potential change. Impedance decreased while potential became more positive, impedance increased while potential became more negative [28-31]. Therefore, each step of assembly process possessed different shape.

Fig. 3

3.4. Amplification of ΔI and impedance

The process of the successive impedance amplification of the impedance enhancer can be described as follows: (1) the carbon spheres can increase ΔI due to their poor conductivity and can absorb Pb^{2+} through electrostatic interaction; (2) Pb^{2+} and sodium tartrate can react to produce a sodium tartrate gel to enhance impedance and, thus, doubles ΔI. The current signals were recorded with the optimum testing conditions. In order to demonstrate the peptide can be cleaved by MMP-2, the modified electrodes were incubated with and without 1 ng mL^{-1} MMP-2. The ΔI (ΔI =I - I_0, where I and I_0 corresponds to the electrochemical signal of the biosensor incubated before and after 1 ng mL^{-1} MMP-2, respectively) was about 27 μA (**Fig. 4A**). To demonstrate the functions of successive enhancements of impedance, the biosensor with CS-AuNPs-Pb was incubated before and after 1 ng mL^{-1} MMP-2. The ΔI was increased to 150 μA (**Fig. 4B**). To investigate the function of the ST-gel, 2.0 mM ST acetate buffer solution (pH 6.0) was added in the proposed biosensor for 1 h to coat electrodes with the ST-gel, which were then incubated before and after 1 ng mL^{-1} MMP-2. As a result, the ΔI increased even more to 310 μA (**Fig. 4C**). These results indicate that the ΔI was enhanced through successive increments of impedance, which can improve the analytical performance of the biosensor.

Fig. 4

3.5. Analytical performance and reliability of the biosensor

The analytical performance of biosensor was recorded by SWV responses. With the increases of MMP-2, the current signal increased (**Fig. 5A**). This biosensor exhibited a wide linear relation between 1 pg mL^{-1} and 1 μg mL^{-1} (the low detection limit of 0.4 pg mL^{-1} (S/N=3)) (**Fig. 5B**), which is wide enough to directly detect MMP-2 in human serum. In order to validate the reliability and accuracy of the proposed biosensor, ten serum samples without dilution were directly analysed, and these results were

compared with the standard addition method tests. The relative standard error was less than 10%, indicating good reliability of the biosensor **(Table 1)**.

Fig. 5

Table 1

3.6. Evaluation of selectivity, reproducibility, and stability of this biosensor

To confirm the selectivity of the biosensor, ascorbic acid (AA), uric acid (UA), carcino-embryonic antigen (CEA), alpha fetoprotein (AFP), and prostate specific antigen (PSA), and matrix metalloproteinase-7 (MMP-7) were used as substitutes to MMP-2. Compared to the blank test (no target molecule), no obvious change in the current signal was observed when the biosensor was incubated with AA (20 ng mL^{-1}), UA (20 ng mL^{-1}), CEA (20 ng mL^{-1}), AFP (20 ng mL^{-1}), PSA (20 ng mL^{-1}), and MMP-7 (20 ng mL^{-1}). However, when MMP-2 was added into the substitutes, the current responses of the samples containing MMP-2 were almost the same regardless of the presence or absence of the substitutes. These results suggest that the proposed biosensor has a good specificity for MMP-2 **(Fig. S5)**. To measure the reproducibility of the biosensor, five samples (1 ng mL^{-1}) were tested. The relative standard error of the five electrodes was about 5%, suggesting good reproducibility of the proposed biosensor. Furthermore, the biosensor was stored at 4 °C for four weeks and its electrochemical signal was tested to examine its stability. The change in current signal was less than 10%, revealing good stability. Compared with previous reports, the proposed biosensor with the impedance-enhancer exhibits a wider detection range and higher sensitivity (Table 2). In order to investigate the accuracy of the proposed biosensor in clinical application, twelve clinical serum samples containing MMP-2 were analysed. The obtained results were compared with ELISA tests (Table 3).

Table 2

Table 3

4. Conclusion

In summary, an amperometric biosensor was developed using polyaniline gel based substrate and a novel impedance enhancer (CS-AuNPs-Pb^{2+}). Compared with other amperometric bioassays, the highlights of this work can be summarized as follows: (1) Multiple impedance amplification strategy was introduced to achieve good analytical performance. (2) CS-AuNP-Pb as a novel probe was synthesized by a one pot method for detection of tumor marker, which exhibited high sensitivity and a wide linear range. This proposed method was further used to analyse MMP-2 in human serum and demonstrated good consistency with ELISA tests. For future industrial application, the stepwise modification process and detection process can be separated. Modification process can be conducted in a kit, the analytical process can operated on the electrode to obtain more reliable results. Overall, this proposed strategy will be of significance in the design of other ultrasensitive biosensing platforms.

Acknowledgments

This research was financed by grants from the National Natural Science Foundation of China (21673143), Natural Science Foundation of Beijing Municipality (2172016), and Capacity Building for Sci-Tech Innovation-Fundamental Scientific Research Funds (19530050179).

Compliance with ethical standards

The author(s) declare that they have no competing interests.

References

[1] D. Wang, Y.L. Yuan, Y.N. Zheng, Y.Q. Chai, R. Yuan, An electrochemical peptide cleavage-based biosensor for matrix metalloproteinase-2 detection with

exonuclease III-assisted cycling signal amplification, Chem. Commun. 52 (2016) 5943-5945.

[2] P. Jing, H.Y. Yi, S.Y. Xue, R. Yuan, W.J. Xu, A 'signal on-off' electrochemical peptide biosensor for matrix metalloproteinase 2 based on target induced cleavage of a peptide, RSC Adv. 5 (2015) 65725-65730.

[3] B.B Kou, L. Zhang, H. Xie, D. Wang, Y.L. Yuan, Y.Q. Chai, R. Yuan DNA enzyme-decorated DNA nanoladders as enhancer for peptide cleavage-based electrochemical biosensor, ACS Appl. Mater. Interfaces 8 (2016)22869-22874.

[4] H.Q. Wang, Z.F. Ma, A novel strategy for improving amperometric biosensor sensitivity using dual-signal synergistic effect for ultrasensitive detection of matrix metalloproteinase-2, Sens. Actuators, B: Chem. 226 (2018) 46-51.

[5] G.H. Yang, L.L.Li, R.K. Rana, J.J. Zhu, Assembled gold nanoparticles on nitrogen-doped graphene for ultrasensitive electrochemical detection of MMP-2" Carbon 61 (2013) 357-366.

[6] B.B. Kou, Y.Q. Chai, Y.L. Yuan, R. Yuan, PtNPs as scaffolds to regulate interenzyme distance for construction of efficient enzyme cascade amplification for ultrasensitrive electrochemical detection of MMP-2, Anal. Chem. 89 (2017) 9383-9387.

[7] H.Q. Wang, Z.F Ma, Simultaneous detection of multiple tumor markers by label-free electrochemical immunoassay using chip-like glass carbon electrodes, Sens. Actuators, B: Chem. 256 (2018) 402-407.

[8] Z.X. Tang, Y. Fu, Z.F. Ma, Multiple signal amplification strategies for ultrasensitive label-free electrochemical immunoassay for carbohydrate antigen 24-2 based on redox hydrogel. Biosens. Bioelectron. 91 (2017) 299-305.

[9] Z.X. Tang, Z.F. Ma, Multiple functional strategies for amplifying sensitivity of amperometric immunoassay for tumor markers: A review. Biosens. Bioelectron. 98 (2017) 100-112.

[10] Z.X. Tang, L.Y. Wang, Z.F. Ma, Triple sensitivity amplification for ultrasensitive electrochemical detection of prostate specific antigen. Biosens. Bioelectron. 92 (2017) 577-582.

[11] H.Q. Wang, Z.F Ma, A cascade reaction signal-amplified amperometric biosensor platform for ultrasensitive detection of tumour marker, Sens. Actuators, B: Chem. 254 (2018) 642-647.

[12] Q. Zhu, Y. Chai, Y. Zhuo, R. Yuan, Ultrasensitive simultaneous detection of four biomarkers based on hybridization chain reaction and biotin-streptavidin signal amplification strategy, Biosens. Bioelectron. 68 (2015) 42-48.

[13] F.J. Arévaloa, G.A. Messina, P.G. Molinaa, M.A. Zóna, J. Raba, H. Fernández, Determination of progesterone (P4) from bovine serum samples using a microfluidic immunosensor system, Talanta 80 (2010) 1986-1992.

[14] N. Li, Y. Wang, Y. Li, W. Cao, H. Ma, D. Wu, B. Du, Q. Wei, A label-free electrochemical immunosensor based on Au@Pd/Ag yolk–bimetallic shell nanoparticles and amination graphene for detection of nuclear matrix protein 22, Sens. Actuators, B: Chem. 202 (2014) 67-73.

[15] Y. Du, Reagentless, ratiometric electrochemical DNA sensors with improved robustness and reproducibility, Anal. Chem. 86 (2014) 8010-8016.

[16] L. Wu, X.H. Zhang, W. Liu, E.H. Xiong, J.H. Chen, Sensitive electrochemical aptasensor by coupling “signal-on” and “signal-off” strategies. Anal. Chem. 85 (2013) 8397-8402.

[17] H.Q. Wang, Z.F. Ma, "Off-on" signal amplification strategy amperometric immunosensor for ultrasensitive detection of tumour marker. Biosens. Bioelectron. 132 (2019) 265-270.

[18] S.I. Stoeva, J.S. Lee, J.E. Smith, S.T. Rosen, C.A. Mirkin, Multiplexed detection of protein cancer markers with biobarcoded nanoparticle probes, J. Am. Chem. Soc. 128 (2006) 8378-8379.

[19] Y. Cheng, F.J. Huang, X.H. Min, P.C. Gao, T.C. Zhang, X.C. Li, B.F. Liu, Y.N. Hong, X. D. Lou, F. Xia, Protease-responsive prodrug with aggregation-induced emission probe for controlled drug delivery and drug release tracking in living cells, Anal. Chem. 88 (2016) 8913-8919.

[20] H.Y. Jia, P.C. Gao, H.M. Ma, D. Wu, B. Du, Q. Wei, Preparation of Au–Pt nanostructures by combining top-down with bottom-up strategies and application in label-free electrochemical immunosensor for detection of NMP22. Bioelectrochemistry 101 (2015) 22-27.

[21] Y. Zheng, Z.F. Ma, Dual-reaction triggered sensitivity amplification for ultrasensitive peptide-cleavage based electrochemical detection of matrix metalloproteinase-7, Biosens. Bioelectron. 108 (2018) 46-52.

[22] Y. Zheng, L.H. Zhao, Z.F. Ma, pH responsive label-assisted click chemistry triggered sensitivity amplification for ultrasensitive electrochemical detection of carbohydrate antigen 24-2, Biosens. Bioelectron. 115 (2018) 30-36.

[23] F.B. Pei, P. Wang, E.H. Ma, Q.S Yang, H.X. Yu, C.X. Gao, Y.Y. Li, Q. Liu, Y.H. Dong, A sandwich-type electrochemical immunosensor based on RhPt NDs/NH_2-GS and Au NPs/PPy NS for quantitative detection hepatitis B surface antigen. Bioelectrochemistry 126 (2019) 92-98.

[24] J. Zhou, L. Du, L. Zou, Y. Zou, N. Hu, P. Wang, An ultrasensitive

electrochemical immunosensor for carcinoembryonic antigen detection based on staphylococcal protein A-Au nanoparticle modified gold electrode, Sens. Actuators, B: Chem. 197 (2014) 220-227.

[25] M. Bauza, G. Ibanez, R. Tauler, A. Olivieri, Sensitivity equation for quantitative analysis with multivariate curve resolution-alternating least-squares: theoretical and experimental approach, Anal. Chem. 84 (2012) 8697-8706.

[26] Q. Zeng, J. Cheng, L. Tang, X. Liu, Y. Liu, J. Jiang, Self-assembled grapheme-enzyme hierarchical nanostructures for electrochemical biosensing, Adv. Funct. Mater. 20 (2010) 3366-3372.

[27] H.Q. Wang, H.L. Han, Z.F. Ma, Conductive hydrogel composed of 1,3,5-benzenetricarboxylic acid and Fe^{3+} used as enhanced electrochemical immunosensing substrate for tumor biomarker. Bioelectrochemistry 114 (2017) 48-53.

[28] A.S. Sarac, M. Ates, B. Kilic, Electrochemical Impedance Spectroscopic Study of Polyaniline on Platinum, Glassy Carbon and Carbon Fiber Microelectrodes, Int. J. Electrochem. Sci. 3 (2008) 777-786.

[29] A. Singh, S.K. Pasha, P. Manickam, S. Bhansali, Single-domain antibody based thermally stable electrochemical immunosensor, Biosens. Bioelectron. 83 (2016) 162-168.

[30] H. Wang, Y. Zhang, H. Li, B. Du, H.M. Ma, D. Wu, Q. Wei, A silver-palladium alloy nanoparticle-based electrochemical biosensor for simultaneous detection of ractopamine, clenbuterol and salbutamol, Biosens. Bioelectron. 49 (2013) 14-19.

[31] S.M. Liu, R. Yuan, Y.Q. Chai, H.L. Su, A label-free amperometric immunosensor based on horseradish peroxidase functionalized carbon nanotubes and bilayer gold nanoparticles, Sens. Actuators, B: Chem. 156 (2011) 388-394.

[32] S.Y. Li, L.H. Liu, H. Cheng, B. Li, W.X. Qiu, X.Z. Zhang, A dual-FRET-based fluorescence probe for the sequential detection of MMP-2 and caspase-3, Chem. Commun. 51 (2015) 14520-14523.

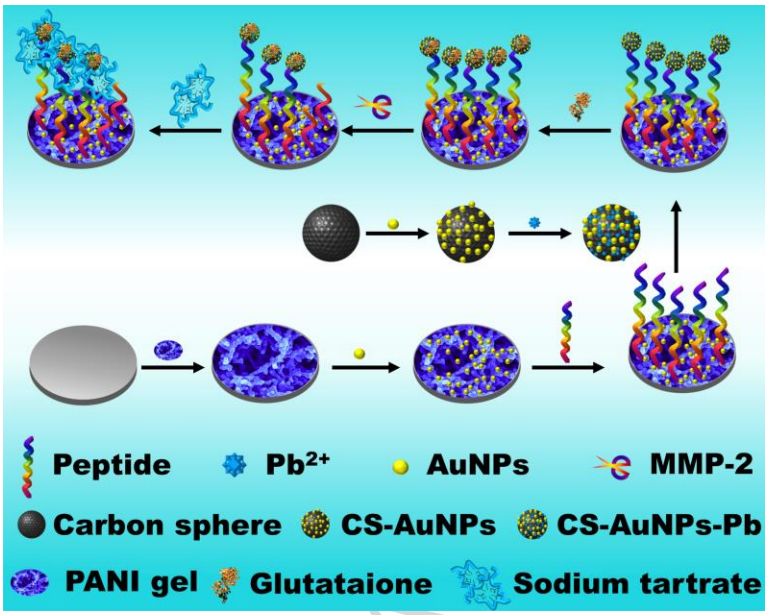

Schematic 1. Schematic illustration of the successive impedance enhancement for ultrasensitive amperometric biosensor.

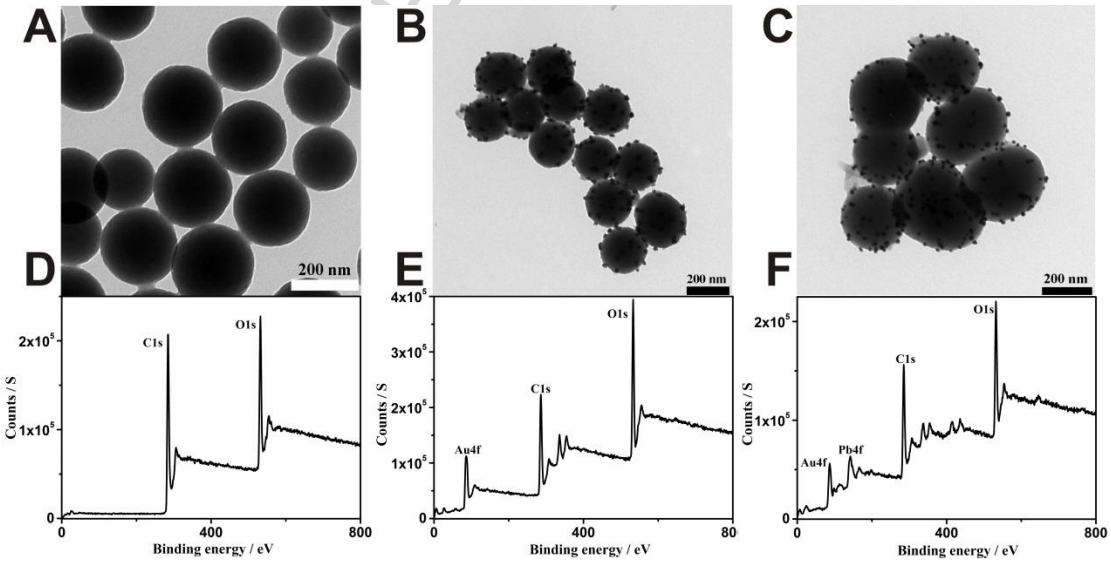

Fig. 1. Characterization of CS-AuNP-Pb nanocomposites. SEM images of CS particles (A), CS-AuNP particles (B), CS-AuNP-Pb nanocomposites (C). XPS of CS particles (D), CS-AuNP particles (E), CS-AuNP-Pb nanocomposites (F).

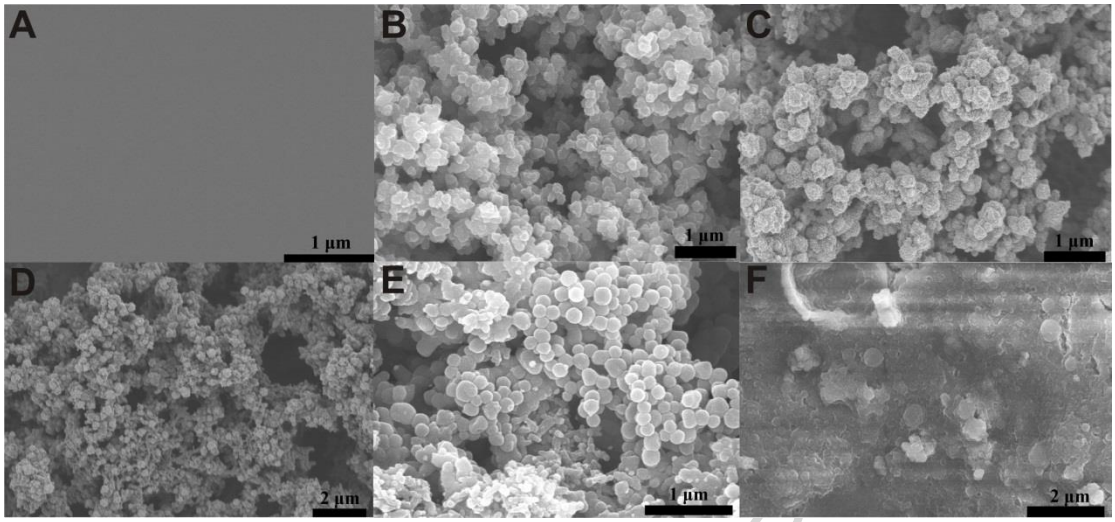

Fig. 2. SEM micrographs of bare GCE (A), PAn-gel/GCE (B), AuNP/PAn-gel/GCE (C), peptides/AuNP/PAn-gel/GCE (D), CS-AuNP-Pb /peptides/AuNP/PAn-gel/GCE (E), and ST-gel/CS-AuNP-Pb /peptides/AuNP/PAn-gel/GCE (F).

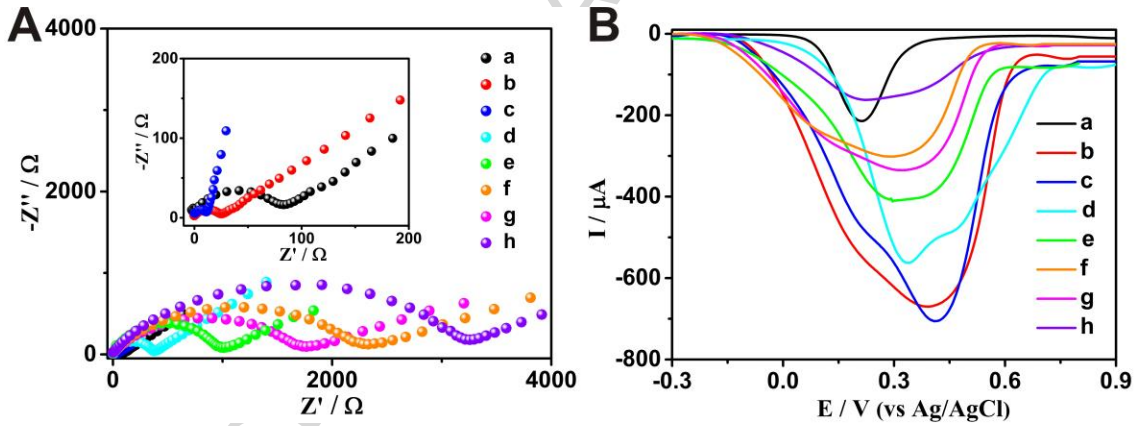

Fig. 3. EIS (A) and SWV (B) of different modified electrodes in 0.01 M phosphate buffered solution containing 5.0 mM $[Fe(CN)_6]^{4-/3-}$ and 0.1 M KCl (pH=7.4): bare GCE (a), PAn-gel/GCE (b), AuNP/PAn-gel/GCE (c), peptides/AuNP/PAn-gel/GCE (d), CS-AuNP-Pb/peptides/AuNP/PAn-gel/GCE (e), further treated by glutathione (f), 1 ng mL^{-1} MMP-2 (g), ST-gel/CS-AuNP-Pb /peptides/AuNP/PAn-gel/GCE (h).

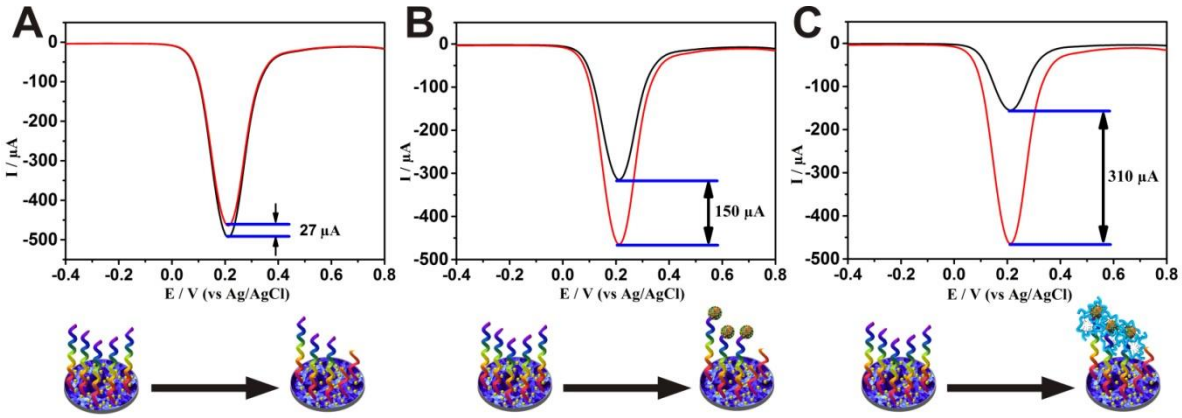

Fig. 4. The comparison of SWV current signal differences: the biosensor without successive enhancement of impedance to improve ΔI (A), the biosensor only treated with CS-AuNP-Pb (B) and the biosensor further treated with ST-gel (C). The biosensor was incubated with 1 ng mL^{-1} MMP-2 (black lines) and with 0 ng mL^{-1} MMP-2 (red lines) (in 0.01 M phosphate buffered solution containing 5.0 mM $[Fe(CN)_6]^{4-/3-}$ and 0.1 M KCl (pH=7.4).

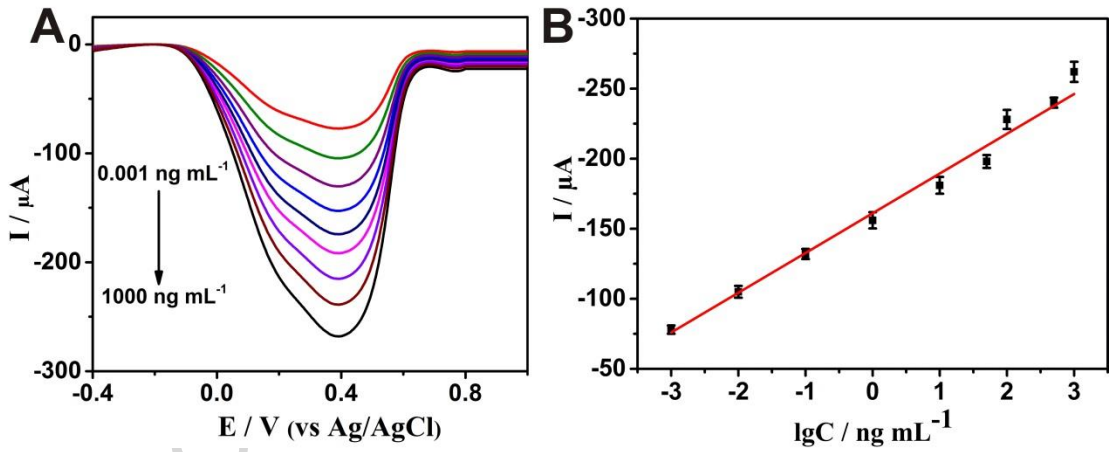

Fig. 5. SWV responses of electrochemical immunoassay in 0.01 M phosphate buffered solution containing 5.0 mM $[Fe(CN)_6]^{4-/3-}$ and 0.1 M KCl (pH=7.4), curves a-i correspond to MMP-2 at the concentrations from 1 pg mL^{-1} to 1000 ng mL^{-1} (A). The calibration plot between the SWV peak current and the logarithm values of MMP-2 concentrations. Error bars represent standard deviation (n=3), the regression equation is y = -28.37x-161.07, R^2 = 0.996 (B).

Table 1. Determination of MMP-2 added in human blood serum with the proposed biosensor (n=3).

Sample	Added MMP-2 (ng mL^{-1})	Found MMP-2 (ng mL^{-1})	Recovery (%)
1	10	411	110
2	10	409	110
3	50	448	104
5	50	453	106
5	100	506	106
6	100	492	92
7	200	610	105
8	200	584	92
9	500	922	104
10	500	920	104

Table 2 A comparison of the performance of the present and referenced biosensors for the detection of MMP-2.

Detection method	Sensitivity $\mu A \cdot (LgC_{MMP-2})^{-1}$	Limit of detection (pg mL^{-1})	Detection linear range (ng mL^{-1})	Reference
amperometry	0.227	0.15	0.0005-50	1
amperometry	8.048	0.32	0.001-10	2
amperometry	14.445	0.05	0.002-20	3
amperometry	43.86		0.01-10	4
amperometry	4.20	0.11	0.0005-50	5
amperometry	0.267	0.003	0.0001-20	6
amperometry	28.4	0.40	0.001-1000	This work

Table 3 Determination of MMP-2 in human serum with the proposed biosensor and

ELISA (n=3).

Sample	Proposed biosensor (ng mL^{-1})	ELISA (ng mL^{-1})	Relative error (%)
1	200.8	204.7	-1.9
2	243.1	221.5	9.8
3	158.2	167.5	-5.6
4	162.6	177.4	-8.3
5	310.4	302.4	2.6
6	150.5	165.2	-8.9
7	179.2	188.8	-5.1
8	102.0	108.2	-5.7
9	149.2	165.2	-9.6
10	191.3	210.6	-4.4
11	121.4	134.5	-9.7
12	178.6	189.6	-5.8

Conflict of Interest

We have no conflicts of interest to declare.

Highlights

1. CS-AuNP-Pb as a novel probe was synthesized for detection of tumor marker.
2. Multiple impedance amplification strategies were applied in the biosensor.
3. Peptide-based amperometric biosensor was used for detection of MMP-2.
4. Pb^{2+} crosslink sodium tartrate forming hydrogel on electrode.
5. The biosensor showed wide linear range from 1 pg mL^{-1} to 1 μg mL^{-1}.